Supplementary Information

Novel human butyrylcholinesterase variants: toward organophosphonate detoxication

Mary Dwyer, Sacha Javor, Daniel A. Ryan, Emily M. Smith, Jun Zhang, John R. Cashman*

*Corresponding Author: John R. Cashman, Human BioMolecular Research Institute, 5310 Eastgate Mall, San Diego CA 92121, Phone: (858) 458-9305, Email: JCashman@hbri.org

Table S1.

Primer	Primer Sequence
hBChE.332S.F	5’-GCTTTTTTAGTCAGCGGTGCTCCTGGC-3’
hBChE.332S.R	5’-GCCAGGAGCACCGCTGACTAAAAAAGC-3’
hBChE.340H.F	5’-GGCTTCAGCAAACACAACAATAGTATC-3’
hBChE.340H.R	5’-GATACTATTGTTGTGTTTGCTGAAGCC-3’
hBChE.332S.340H.F	5’-GCTTTTTTAGTCAGCGGTGCTCCTGGCTTCAGCAAACACAACAAT-3’
hBChE.332S.340H.R	5’-ACTATTGTTGTGTTTGCTGAAAGGAGCACCGCTGACTAAAAAAGC-3’

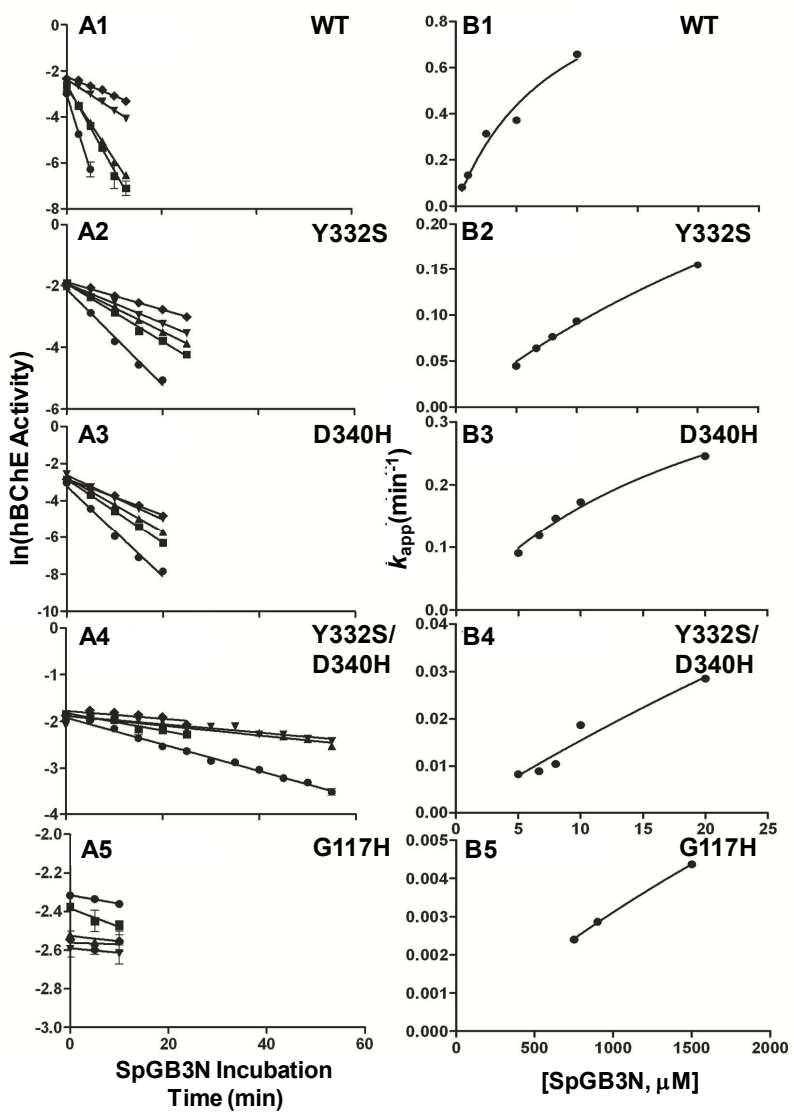

Figure S1. (A) Plots of residual hBChE activity versus incubation time with *S*PGB3N: WT (**A1**) and Y332S (**A2**), D340H (**A3**), Y332S/D340H (**A4**) and G117H (**A5**) variant hBChE inhibition by *S*PGB3N. WT and variant hBChE was incubated with a concentrations of *S*PGB3N (i.e., ♦0.5 μM, ▼1 μM, ▲2.5 μM, ■5 μM, ●10 μM *S*PGB3N for WT, ♦5 μM, ▼6.67 μM, ▲8 μM, ■10 μM, ●20 μM *S*PGB3N for Y332S, D340H, and Y332S/D340H, ♦500 μM, ▼750 μM, ▲900 μM, ■1000 μM, ●1500 μM *S*PGB3N for G117H) for the indicated period of time. The percent remaining activity post-inhibition was determined by the Ellman assay. The natural log of activity was plotted as a function of the duration of enzyme inhibition versus inhibitor concentration and fit to a linear regression line. The best-fit slope values defined the apparent rate constants k_{app}. **(B)** Replot of k_{app} versus inhibitor concentration for the incubations of WT (**B1**), Y332S (**B2**), D340H (**B3**), Y332S/D340H (**B4**) and G117H (**B5**) in the presence of *S*PGB3N. The best-fit k_{app} values were derived from slopes of linear regression analysis as shown in (**A**). Data were fit to the equation of $k_{app} = k_2[S_PGB3N]/(K_D + [S_PGB3N])$.

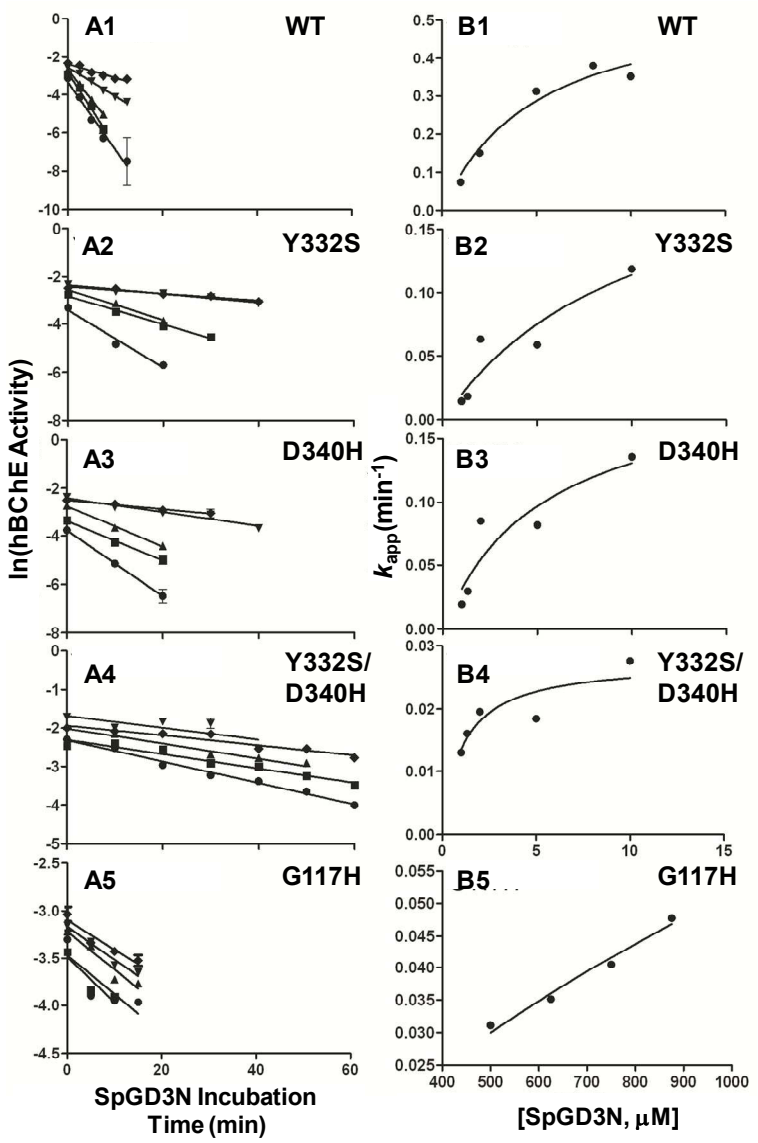

Figure S2. (A) Plots of residual hBChE activity versus incubation time with *S*PGD3N: WT (**A1**) and Y332S (**A2**), D340H (**A3**), Y332S/D340H (**A4**), and G117H (**A5**) variant hBChE inhibition by *S*PGD3N. WT and variant hBChE was incubated with a concentration range of *S*PGD3N (i.e., ♦1 μM, ▼2 μM, ▲5 μM, ■8 μM, ●10 μM *S*PGD3N for WT, ♦1 μM, ▼1.33 μM, ▲2 μM, ■5 μM, ●10 μM *S*PGD3N for Y332S, D340H, and Y332S/D340H, ♦500 μM, ▼625 μM, ▲750 μM, ■875 μM, ●1000 μM *S*PGD3N for G117H) for the indicated period of time. The percent remaining activity post-inhibition was determined by the Ellman assay. The natural log of the activity was plotted as a function of the duration of enzyme inhibition versus inhibitor concentration and fit to a linear regression line. The best-fit slope values defined the apparent rate constants k_{app}. **(B)** Replot of k_{app} versus inhibitor concentration for the incubations of WT (**B1**), Y332S (**B2**), D340H (**B3**), Y332S/D340H (**B4**) and G117H (**B5**) with *S*PGD3N. The best-fit k_{app} values were derived from slopes of linear regression analysis as shown in (**A**). Data were fit to the equation of $k_{app} = k_2[S_PGD3N]/(K_D + [S_PGD3N])$.

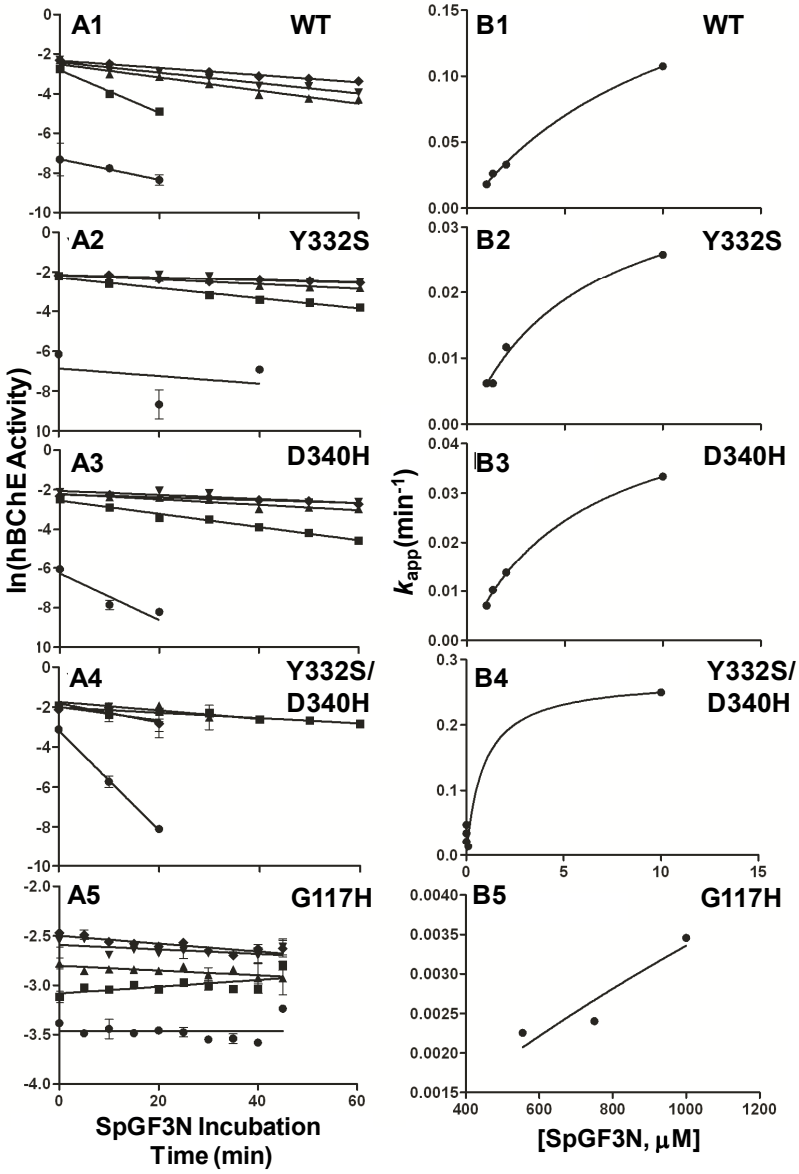

Figure S3. (A) Plots of residual hBChE activity versus incubation time with *S*PGF3N: WT (**A1**) and Y332S (**A2**), D340H (**A3**), Y332S/D340H (**A4**), and G117H (**A5**) variant hBChE inhibition by *S*PGF3N. WT and variant hBChE were incubated with a diverse concentration range of *S*PGF3N (i.e., ♦0.01 μM, ▼0.0133 μM, ▲0.02 μM, ■0.1 μM, ●10 μM *S*PGF3N for WT, Y332S, D340H, Y332S/D340H, ♦500 μM, ▼555 μM, ▲750 μM, ■1000 μM, ●2000 μM *S*PGF3N for G117H) for the indicated period of time. The percent remaining activity post-inhibition was determined by the Ellman assay. The natural log of the activity was plotted as a function of the duration of enzyme inhibition versus inhibitor concentration and fit to a linear regression line. The best-fit slope values defined the apparent rate constants k_{app}. **(B)** Replot of k_{app} versus inhibitor concentration for the incubations of WT (**B1**), Y332S (**B2**), D340H (**B3**), Y332S/D340H (**B4**) and G117H (**B5**) with *S*PGF3N. The best-fit k_{app} values were derived from slopes of linear regression analysis as shown in (**A**). Data were fit to the equation of $k_{app} = k_2[S_PGF3N]/(K_D + [S_PGF3N])$.

A. **B.**

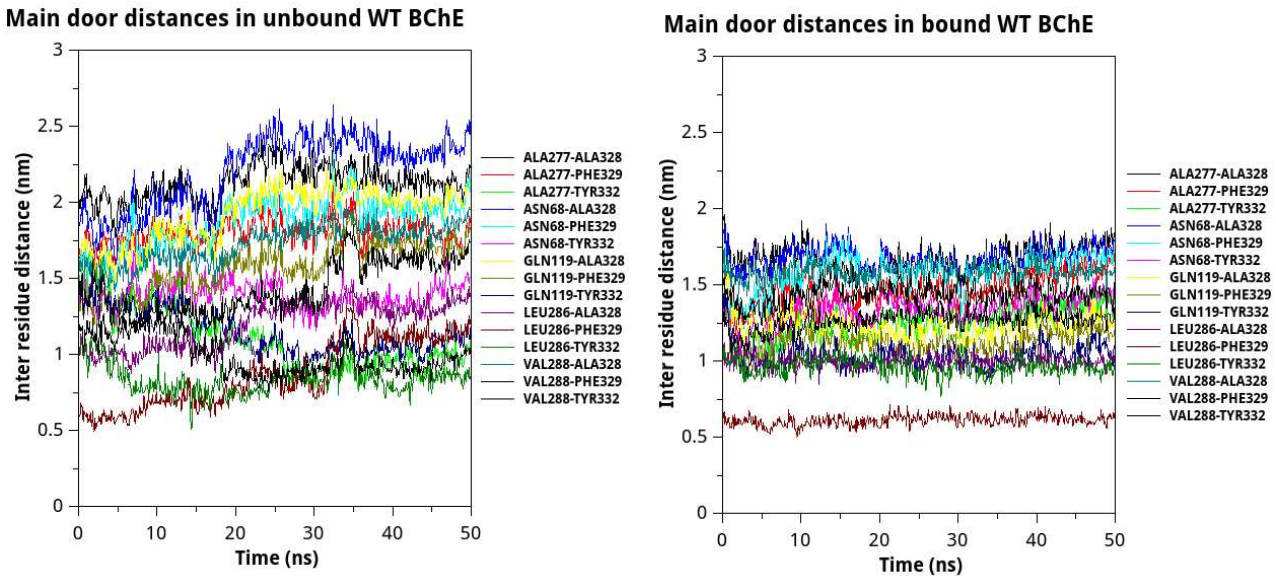

Figure S4. A plot of distance between the center of mass of pairs of residues (V288, Q119, L286, N68, A277 and A328, F329, Y332) on each side of hBChE "main door" as a function of time for molecular dynamics simulations of the WT hBChE in the presence or absence of *S*PGB3N bound to the active site.

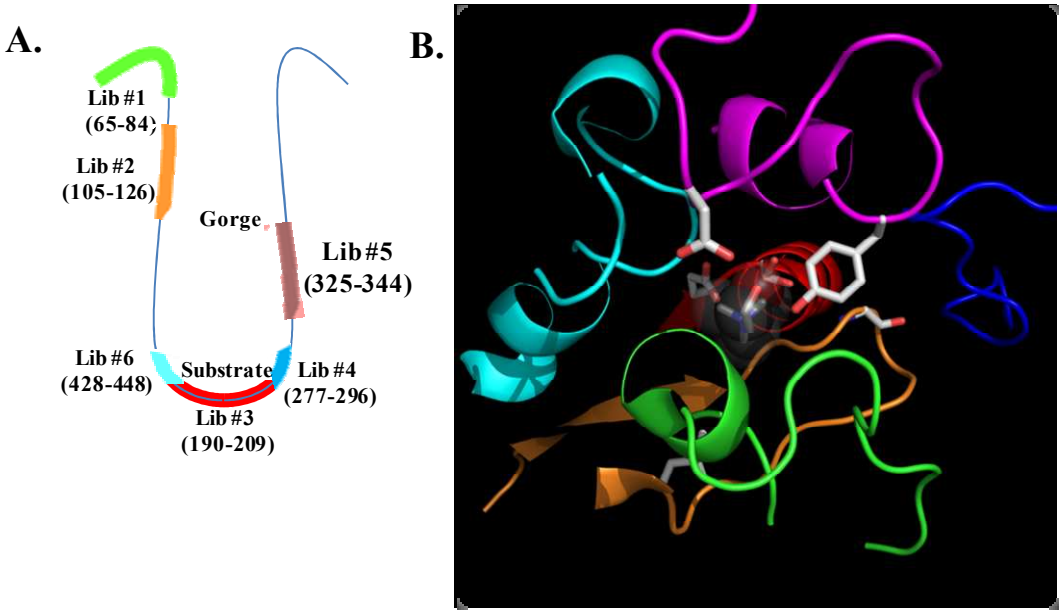

Figure S5.[4] Depiction of mutation libraries of hBChE. (**A)** Cartoon showing the active site of hBChE. Each color represents a corresponding peptide sequence that was constructed in individual libraries: green, library #1; orange, library #2; pink, library #3; blue, library #4; brown, library #5; aqua, library 6. (**B)** Three-dimensional view of the active site of hBChE.

4. Zhang, J., Chen, S., Ralph, E. C., Dwyer, M., and Cashman, J. R. (2012) Identification of human butyrylcholinesterase organophosphate-resistant variants through a novel mammalian enzyme functional screen, *J Pharmacol Exp Ther 343*, 673-682.